Acoustic Assessment of a Konjac–Carrageenan Tissue-Mimicking Material at 5–60 MHz

Ultrasound in Med. & Biol., Vol. 40, No. 12, pp. 2895–2902, 2014

0301-5629/$ - see front matter

http://dx.doi.org/10.1016/j.ultrasmedbio.2014.07.006

● *Original Contribution*

ACOUSTIC ASSESSMENT OF A KONJAC–CARRAGEENAN TISSUE-MIMICKING MATERIAL AT 5–60 MHZ

David A. Kenwright,* Neelaksh Sadhoo,† Srinath Rajagopal,† Tom Anderson,* Carmel M. Moran,* Patrick W. Hadoke,* Gillian A. Gray,* Bajram Zeqiri,† and Peter R. Hoskins*

*Centre for Cardiovascular Science, University of Edinburgh, Edinburgh, United Kingdom; and †Acoustics and Ionising Radiation Division, National Physical Laboratory, Teddington, United Kingdom

(*Received* 31 *January* 2014; *revised* 3 *July* 2014; *in final form* 11 *July* 2014)

Abstract—The acoustic properties of a robust tissue-mimicking material based on konjac–carrageenan at ultrasound frequencies in the range 5–60 MHz are described. Acoustic properties were characterized using two methods: a broadband reflection substitution technique using a commercially available preclinical ultrasound scanner (Vevo 770, FUJIFILM VisualSonics, Toronto, ON, Canada), and a dedicated high-frequency ultrasound facility developed at the National Physical Laboratory (NPL, Teddington, UK), which employed a broadband through-transmission substitution technique. The mean speed of sound across the measured frequencies was found to be 1551.7 ± 12.7 and 1547.7 ± 3.3 m s^{-1}, respectively. The attenuation exhibited a non-linear dependence on frequency, f (MHz), in the form of a polynomial function: $0.009787f^2 + 0.2671f$ and $0.01024f^2 + 0.3639f$, respectively. The characterization of this tissue-mimicking material will provide reference data for designing phantoms for preclinical systems, which may, in certain applications such as flow phantoms, require a physically more robust tissue-mimicking material than is currently available. (E-mail: david.kenwright@ed.ac.uk) © **2014 World Federation for Ultrasound in Medicine & Biology.**

Key words: **Ultrasound, High frequency, Tissue-mimicking material, Speed of sound, Attenuation, Preclinical ultrasound.**

INTRODUCTION

High-frequency ultrasound is an increasingly used tool for life science applications, particularly in preclinical imaging. Protocols have long existed for validating ultrasound measurements for clinical scanners (Hoskins 2008), and recent work has addressed higher-frequency systems (Moran et al. 2011). With increased frequency come further challenges to quality assurance, such as the decrease in penetration depth and issues related to transducer design (Goertz et al. 2002; Xu et al. 2008), and as such, systems suitable for conventional low-frequency clinical ultrasound may not be appropriate for preclinical investigations. Therefore, novel materials and methodologies are required specific to high-frequency ultrasound (e.g., Cannon et al. 2011; Yang et al. 2013).

Tissue-mimicking materials (TMMs) are designed to act as a substitute for soft tissue, with approximately equivalent values for speed of sound and acoustic attenuation (International Electrotechnical Commission [IEC] 2001; Hoskins 2008). The advantage of TMMs is that they can be manufactured in a controlled manner with well-characterized, highly reproducible and uniform acoustic properties. As such they are extensively used in ultrasound quality control, for example, in imaging where they can be embedded or molded into structures for imaging phantoms (Foster et al. 2009; King et al. 2011; Moran et al. 2011; Wells 2006) or for use in Doppler phantoms (Hoskins 2011; Ramnarine et al. 2001; Rickey 1995; Steel and Fish 2003; Yang et al. 2013).

The acoustic properties of many TMMs have been investigated previously (Brewin et al. 2008; Browne et al. 2003; King et al. 2011; Madsen et al. 1986, 1998), with increasing interest in the high-frequency region above 25 MHz (Cannon et al. 2011; Ryan and

Address correspondence to: David Kenwright, Centre for Cardiovascular Science, University of Edinburgh, Queen's Medical Research Institute, 47 Little France Crescent, Edinburgh EH164 TJ, UK. E-mail: david.kenwright@ed.ac.uk

This work was supported by the British Heart Foundation Project Grant PG/10/012/28201.

Foster 1997; Sun et al. 2012). Detailed knowledge of these properties is required to ensure the consistency of measurements carried out between different systems and to ensure that further uncertainties are not introduced, such as artifacts from a speed of sound mismatch. As high-frequency ultrasound becomes more prevalent, there will be a growing need for appropriate tissue-mimicking materials to be characterized for use in phantoms.

The IEC developed an agar-based TMM (IEC 2001; Teirlinck et al. 1998), which has subsequently become widely used in clinical test objects and has recently been acoustically characterized at high frequencies to assess its suitability for preclinical applications (Sun et al. 2012). However, the structural integrity of this TMM has been found to be a limiting factor in the design of wall-less flow phantoms for clinical use, as rupturing occurs at points of high pressure (Meagher et al. 2007). We have found this to also be the case for a wall-less flow phantom designed to replicate preclinical applications, where the phantom was modeling a rat artery at a 2-mm depth. The IEC agar-based TMM would rupture because of the pressure when blood-mimicking fluid was passed through at biologically equivalent flow velocities (20–80 cm s^{-1}). Therefore, an alternative TMM is required for wall-less preclinical flow phantoms.

A physically stronger TMM based on konjac–carrageenan (KC-TMM) has been reported by Meagher et al. (2007). The KC-TMM was able to withstand physiologic pressures at which the agar-TMM would fail and, as such, is potentially more suitable for the development of wall-less flow phantoms for preclinical use. The acoustic properties were briefly reported, but only at a frequency of 5 MHz. The aim of the present study was to investigate the speed of sound and attenuation of the KC-TMM over the frequency range 5–60 MHz, thereby covering frequencies used by commercial preclinical scanners.

METHODS

The attenuation and speed of sound in the KC-TMM was determined using different methods at two facilities. The first employed a broadband reflection substitution technique using a Vevo 770 preclinical ultrasound scanner (FUJIFILM VisualSonics Inc., Toronto, ON, Canada) at the University of Edinburgh preclinical imaging facility. The second system employed was a dedicated high-frequency characterization facility, developed at the Acoustics Group of the National Physical Laboratory (NPL, Teddington, UK) and founded on a through-transmission substitution technique. In our methods, we use the generic term *attenuation* with the knowledge that this is a combination of absorption and backscatter.

Manufacture of the KC-TMM test cells

The components of the KC-TMM and their percentages by weight are given in Table 1. KC-TMM was prepared according to the recipe described by Meagher et al. (2007). Polyvinyl chloride (PVC) cylinder rings with an inner diameter of 4.8 cm and a thickness of 2.00 ± 0.02 or 4.00 ± 0.02 mm (mean ± standard deviation of five micrometer measurements) acted as molds for the TMM. (Note that the thickness of the TMM is calculated independently of the PVC rings, as described below.) A taut layer of ~18-μm-thick Saran wrap (SC Johnson, Racine, WI, USA) was glued to the lower surface of the PVC ring with Araldite Rapid (Huntsman Advanced Materials, Basel, Switzerland). With the Saran wrap-covered side resting on a flat sheet of rigid Perspex, the molten TMM was poured into the PVC ring and carefully (to prevent the introduction of air bubbles) pressed flat with a second weighted sheet of Perspex. Once the TMM had cooled and congealed, the upper Perspex sheet was removed, and a small volume (~0.2 mL) of 10% glycerol solution was applied with a syringe and spread over the KC-TMM before sealing with a glued layer of Saran wrap on the upper surface of the PVC ring. The glycerol solution was used to provide good acoustic coupling between the sample and the Saran wrap. On visual inspection, there was no significant contraction of the TMM during cooling. Sealing the cells in Saran wrap prevented the water from the measurement tank from coming into contact with the KC-TMM and changing its composition. An example test cell is illustrated in Figure 1.

Eight test cells (four of each thickness) were measured at the two facilities. The NPL facility used the different thicknesses to correct for the transmission loss occurring at the water–Saran–TMM and TMM–Saran–water interfaces of the test cell (Zeqiri et al. 2010b). For the Vevo 770 measurements, a 2-mm-thick water test cell, filled with degassed distilled water in place of the KC-TMM, was used to correct for the Saran wrap. The differences between the interfacial transmission losses for water–Saran–water and water–Saran–TMM were calculated and corrected according to the impedance mismatches of the materials. The frequency-

Table 1. Percentage weight composition of the konjac–carageenan tissue-mimicking material

Component	Weight %
De-ionized water	84
Glycerol	10
Silicon carbide 400 grain	0.53
Aluminum powder (3 μm)	0.96
Aluminum powder (0.3 μm)	0.89
Konjac powder	1.5
Carageenan powder	1.5
Potassium chloride	0.7

Fig. 1. Example konjac–carrageenan tissue-mimicking test cell.

dependent transmission loss of the membrane material was calculated using the transmission model equation described in Wear et al. (2005) and employed the following physical properties of Saran wrap (low-density polyethylene): speed of sound = 2100 ms^{-1}; density = 925 kg m^{-3}. The maximum difference in transmission loss for water-Saran-water and water-Saran-TMM was 0.42 dB at 33 MHz, dropping to 0.06 dB at 10 MHz and 0.01 dB at 60 MHz.

Acoustic measurements using Vevo preclinical ultrasound scanner

The Vevo 770 measurements involved a broadband reflection substitution technique (American Institute of Ultrasound in Medicine 1995; Sun et al. 2012). Four different single-element transducers were used; details of the 3-dB beam widths and focal depths are provided in Table 2. The time delays and magnitudes of the received sound pulses through the KC-TMM sample were compared with those through only water. The effects of the Saran wrap windows were accounted for by comparing the signals with those through the water-filled test cell.

Table 2. Characteristics of the Vevo 770* transducers†(3 dB bandwidth data reproduced from Sun2012)

	Transducer model			
	710B	707 B	704	711
Measured 3-dB bandwidth (MHz)	12–25	17–31	20–40	27–47
Focal length (mm)	15	12.7	6	6

* FUJIFILM VisualSonics, Toronto, ON, Canada.
† Three-decibel-bandwidth data reprinted from Sun et al. (2012).

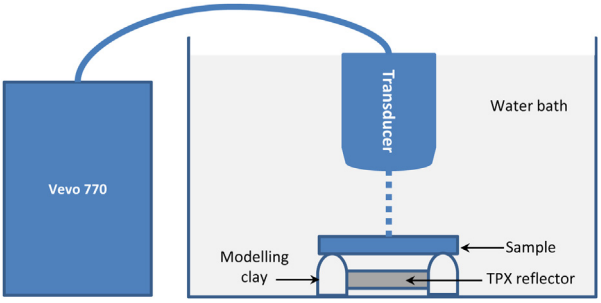

Fig. 2. Schematic of the Vevo 770 (FUJIFILM VisualSonics, Toronto, ON, Canada) setup. TPX = polymethylpentene.

Figure 2 illustrates the experimental setup. A polished polymethylpentene (TPX) reflector (Boedeker Plastics, Shiner, TX, USA) was placed at the bottom of a water tank filled with distilled water, which acted as a reference reflector. The transducers were positioned at a distance from the TPX reflector equal to their focal length (Table 2) to obtain the maximum reference signal. The TMM test cell was placed in the water bath between the transducer and the TPX reflector. The scanner was set to a power output of 10% as a compromise between reducing the generation of non-linear effects and obtaining an adequate signal magnitude (Sun et al. 2012). Temperature was monitored using a physiologic monitoring unit (VisualSonics); all measurements were carried out at 22 ± 1°C.

Measurements with the Vevo scanner were obtained in radiofrequency (RF) mode. 10 lines of RF data were recorded at four independent locations on each test cell. As it was not possible to capture the RF data from the entire image, a region of interest was selected for each of the echoes corresponding to each surface to be measured before acquiring the data. The RF data were downloaded, and calculations were performed using MATLAB 2012b (The MathWorks, Natick, MA, USA).

Speed of sound

The speed of sound, V_{tmm}, was derived from the return times of the peak amplitude of the reflections obtained from the front and rear faces of the test cell and the TPX reflector:

$$V_{tmm} = \left(1 + \frac{T_{wr} - T_3}{T_2 - T_1 + T_{wr} - T_r}\right) V_{water} \quad (1)$$

(for the full derivation, see Sun 2012). The thickness, d_{tmm}, of the TMM sample was then determined by the time-of-flight method described in Kuo et al. (1990), given by the equation.

$$d_{\text{tmm}} = V_{\text{tmm}} \times [T_1 - T_2 - (T_r - T_{\text{wr}})] \quad (2)$$

where time intervals between the transducer and a given surface are: T_1, the upper layer of Saran wrap; T_2, the lower layer of Saran wrap through the test cell; T_3, the TPX reflector through the test cell; T_{wr}, the TPX reflector through the water-filled cell; T_{r} the TPX reflector through water only. V_{water} is the speed of sound in water, at the corresponding recorded temperature (Del Grosso and Mader 1972).

Measurement of attenuation

Attenuation was calculated by measuring the frequency-dependent (f) change in amplitude of the ultrasound waveform between the through-water setup with the water-filled test cell in place, $A_0(f)$, and with the TMM test cell in place, $A_{\text{tmm}}(f)$. The attenuation coefficient, α (dB cm^{-1}), is then defined as.

$$\alpha(f) = \frac{20}{2d_{\text{tmm}}} \log \frac{A_0(f)}{A_{\text{tmm}}(f)} + \alpha_{\text{w}} \quad (3)$$

where d_{tmm} is the sample thickness (in cm). A correction (α_{w}) was applied to account for the attenuation caused by water through the sample thickness by fitting a seventh-order polynomial to the data that appear in Pinkerton (1949).

Acoustic measurements using the NPL system

The NPL material characterization facility implements a broadband through-transmission substitution technique to determine the attenuation and speed of sound (Zeqiri and Bickley 2000; Zeqiri et al. 2010b). A fuller description of the technique and the uncertainties may be found in Rajagopal et al. (2014). The experimental setup is outlined in Figure 3: briefly, a transmitting transducer, the test cell and a receiving transducer were mounted in a test tank filled with de-ionized water. The properties of the test material were calculated relative to values previously established for such distilled, deionized water (Zeqiri et al. 2010b). Each measurement set for acoustic characterization of a sample required the acquisition of two acoustic pulses: through-water transmission

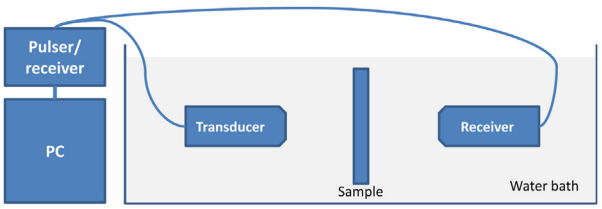

Fig. 3. Schematic of the dedicated high-frequency ultrasound facility developed at the National Physical Laboratory (NPL, Teddington, UK).

("reference" measurement, with sample absent) and through sample, in combination with the measured thickness. Acoustic reflections, monitored by the pulse-echo response of the transmitter originating from the test sample's front and rear surfaces, were used to ensure that the test samples were aligned orthogonally on the transducer axis.

Measurements were carried out with different pairs of transducers to cover high and low ultrasonic frequencies. For the high-frequency measurements, two nominally identical 50-MHz-centered transducers (V358, Olympus NDT, Waltham, MA, USA) acted as transmitter and receiver. For the low-frequency measurements, these were substituted with two transducers centered at 15 MHz (V313, Olympus NDT). In each case, the transmitter and receiver were secured in independent micropositioning mounts with five degrees of freedom (x-, y- and z-axis translation, rotation and tilt), and aligned coaxially along the near-far mechanical axis of the water tank. A default transmitter–receiver separation yielding a 25-μs water path delay was employed, balancing constraints of acceptable signal-to-noise ratio and easy access to the test sample mount.

Test samples were to be mounted perpendicular to the transmitter–receiver acoustic axis, on a Newport 605-4 Series Gimbal Optic Mount (Newport Spectra-Physics Ltd, Didcot, UK) installed at the center of the tank, roughly halfway between the transducers. The gimbal mount allowed independent tilt and rotation of the sample to optimize acoustic reflections from the sample surfaces (Rajagopal et al. 2014).

An Olympus 5073 PR pulser–receiver (Olympus NDT, Waltham, MA, USA) controlled the transmitting and receiving signals. Waveforms were acquired and analyzed by software developed at NPL using LabVIEW (National Instruments, Austin, TX, USA). Waveforms were acquired using a DPO 7254 oscilloscope (Tektronix UK Ltd, Bracknell, UK).

Water temperature was monitored with a UKAS-calibrated IP39 C spirit-in-glass thermometer (G H Zeal, London, UK) placed in the water bath. The water temperature was 21.3 ± 0.1°C for all measurements.

Four independent measurement sets were completed for each sample of KC-TMM, with the sample removed from the tank between sets.

Measurement of speed of sound

Phase velocity in a given KC-TMM (V_{tmm}) sample was calculated using the equation.

$$\frac{1}{V_{\text{tmm}}(f)} = \frac{\varnothing_{\text{tmm}}(f) - \varnothing_{\text{water}}(f) + 2\pi f(t_{\text{tmm}} - t_{\text{saran}})}{2\pi f d_{\text{tmm}}} + \frac{1}{V_{\text{water}}} \quad (4)$$

($Ø_{tmm} - Ø_{tmm}$) is the phase difference obtained by aligning each pulse within its sampling window by shifting the peak positive voltage of the signal to the center of the sampling window and this phase difference is then unwrapped using traditional discontinuity algorithm; t_{tmm} is the time difference between the peaks of the through-sample and through-water pulses within the sampling window; t_{saran} is the time delay introduced by the Saran film, calculated using measured thickness and assuming a velocity of 2100 m s^{-1} (He 2000; Wu 1996); and d_{tmm} is the thickness of the sample, excluding Saran film on either side, measured independently of the PVC ring thickness measurements using a micrometer.

Measurement of attenuation

For each determination of attenuation, we characterized two KC-TMM samples of different thickness and then employed the equation.

$$\alpha_s(f) = \frac{TL_2 - TL_1}{d_2 - d_1} + \alpha_w(f), \quad (5)$$

where $\alpha_s(f)$ is the intrinsic frequency-dependent amplitude-attenuation coefficient (in dB cm^{-1}) in the KC-TMM; d_1 and d_2 are the two measured sample thicknesses; and TL_1 and TL_2 are the transmission/insertion losses for each sample, calculated as a log ratio of voltage-magnitude spectra for through-sample transmission, $U_s(f)$, and reference/water-path transmission, $U_w(f)$:

$$TL = -20 \times \log\left(\frac{U_s(f)}{U_w(f)}\right) \quad (6)$$

For two samples differing only in thickness, these calculations cancel out the transmission losses at the water–Saran–TMM and TMM–Saran–water interfaces.

RESULTS

Table 3 lists the mean speed of sound as calculated for each of the Vevo 770 transducers and the low- and high-frequency measurements from the NPL system. Overall, the mean speed of sound from the Vevo 770 system was 1551.7 ± 12.7 m s^{-1}, and that from the NPL measurements, 1547.7 ± 3.3 m s^{-1}. For the Vevo 770 measurements, the speed of sound was calculated at the central frequency for each transducer, as determined by the manufacturer (Table 3). The NPL measurements having been derived from the phase speed, the speed of sound was determined over a range of frequencies for each transducer. The results for the two systems agree within error bars, and the frequency-dependent dispersion over the frequency range was low, as can be seen in Figure 4. When the individual measurements from both systems were combined, the weighted average speed of sound was 1548 ± 6 m s^{-1} (weighted by the number of measurements at individual frequencies from each system). A paired *t*-test using the mean and standard deviations of the speed of sound at four different frequencies, dictated by the central frequency of the Vevo 770 transducers (Table 3), was used to compare the difference in results between the two measurements systems. The two-tailed *p*-value was 0.30, and therefore, the difference is not considered to be statistically significant.

Table 3. Mean speed of sound of the tissue-mimicking material test cells for the different Vevo 770* transducers and the NPL HF and NPL LF measurements, with the corresponding central frequency or range of frequencies over which the speed of sound was calculated†

Transducer (Central frequency/range)	Speed of sound (m s^{-1})
710B (25 MHz)	1556.9 (8)
707B (30 MHz)	1552 (8)
704 (40 MHz)	1541 (11)
711 (55 MHz)	1558 (16)
NPL LF (5–25 MHz)	1549.1 (0.5)
NPL HF (20–60 MHz)	1546.2 (0.4)

NPL = National Physical Laboratory (NPL, Teddington, UK), HF = high frequency, LF = low frequency.
* FUJIFILM VisualSonics, Toronto, ON, Canada.
† Standard deviations are given in parentheses. Note that for the Vevo 770 transducers, the speed of sound is calculated at a single (central) frequency and averaged across the measurements made on each cell. For the NPL measurements, the speed of sound was calculated across a range of frequencies with each transducer, from which the average and standard deviation were obtained.

Attenuation increased as a function of frequency, as illustrated in Figure 5. A polynomial function was chosen as a fit to the NPL data as a function of frequency, $0.01024f^2 + 0.3639f$ ($R^2 = 0.99$). The Vevo 770 measurements were lower than the NPL measurements, with

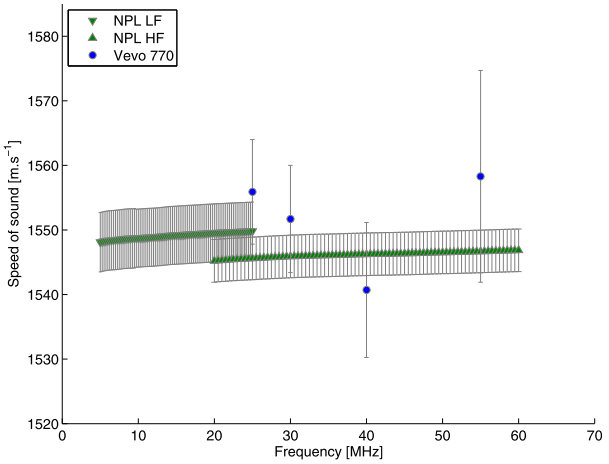

Fig. 4. Speed of sound as a function of frequency. NPL = National Physical Laboratory, HF = high frequency, LF = low frequency.

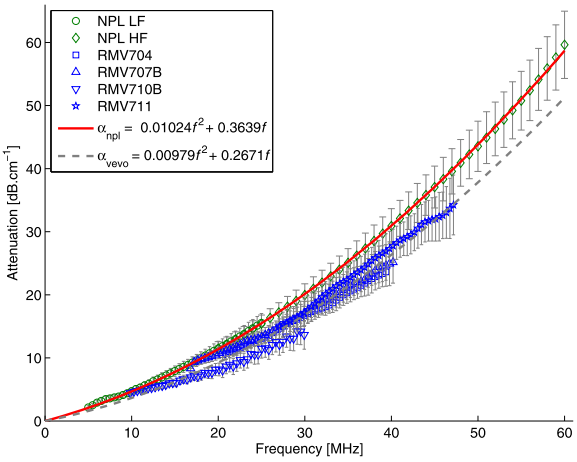

Fig. 5. Attenuation as a function of frequency for the National Physical Laboratory (NPL) and Vevo 770 measurements. A polynomial curve is fitted to the results of each system (α_{npl} and α_{vevo}). HF = high frequency, LF = low frequency.

some variation between the transducers at overlapping frequency intervals. A similar characteristic was observed for the attenuation of the IEC agar-based TMM (Sun 2012). A polynomial function was fitted for the data over all of the Vevo 770 transducers: $0.009787f^2 + 0.2671f$.

DISCUSSION

The measured speed of sound is consistent with the IEC guideline of 1540 m/s ± 1% for a TMM used in a flow Doppler test object. Statistical testing revealed that there was no significant difference between the mean values of the speed of sound measured with the two measurement systems. There is little observed variation across the frequency range; frequency-dependent dispersion is less than 1% over the frequency range 5 to 60 MHz. The theoretical dispersion in sound speed can be calculated from absorption data using the Kramers–Kronig relationship, first described by O'Donnell et al. (1981) with the relationship.

$$\Delta c = c(\omega) - c_0 = \frac{2c_0^2}{\pi}\int_{\omega_0}^{\omega}\frac{\alpha(\omega')}{\omega'^2}d\omega, \qquad (7)$$

where ω is the angular frequency; $\alpha(\omega)$ is the frequency-dependent absorption coefficient of the material whose attenuation is linearly increasing with frequency ($\alpha = af^b$); and $c(\omega)$ and c_0 are, respectively, the sound speed or phase velocity at the frequency of interest and the reference frequency, where $c_0 < c(\omega)$. Using the NPL data for attenuation, we have $\alpha = 0.01024f^2 + 0.3639f$. For the purposes of this analysis, we will assume linearity, that is, $\alpha = 0.3639f$. Employing this relationship to derive the dispersion over the frequency range 5–60 MHz, using eqn (7), yields a predicted increase in speed of sound of 2.5 m s^{-1}. Of course, it is clear from the attenuation results for the KC-TMM that $b > 1$ (approximately 1.3, using a power law fit to the NPL-derived attenuation). However, as indicated by Szabo (1995), the predicted dispersion relative to the O'Donnell model is insensitive to changes in b around $b = 1$. These predictions are clearly consistent with the experimental values of speed of sound presented in this study. It is worth noting that the Rajagopal et al. (2014) study on the agar-TMM predicted a similarly low level of dispersion in sound speed of 6 m s^{-1} over the wider frequency range of 1 to 60 MHz.

Attenuation was calculated using two independent methods. These values are again similar to those for the IEC agar-based TMM, wherein the slope of attenuation increases with increasing frequency. The difference in attenuation values between the two methods, particularly at higher frequencies, could be due to the alignment of the test sample in the acoustic beam (Zeqiri et al. 2010b). The dedicated alignment micropositioning mounts in the NPL system will have reduced the errors in these measurements. The results are in agreement within the uncertainties of the two methods; however, there is a systematic difference. The fundamental difference between the two measurement techniques employed is that the NPL facility uses a piston receiver in through-transmission mode, whereas the Vevo 770 employs a highly focused receiver operating in reflection mode. The difference could be a diffraction artifact, or alternatively, the acoustic pressures generated may be too high such that non-linear losses occur as the waveform propagates through the water.

The difference might also be due to signal-to-noise at higher frequencies, which will tend to suppress the measured attenuation as frequency increases. Noise will effectively boost the signal at a particular frequency, and as the transmitted signal becomes negligible at higher frequencies, the noise will make a bigger contribution to the measured transmission, decreasing the signal-to-noise ratio. Any inherent noise in the system will result in an overestimation of transmission and an underestimation of the derived attenuation. We expect that the signal-to-noise ratio will be poorer for the Vevo 770, which would therefore account for the greater discrepancy in the slope between the two measurement systems, particularly at higher frequencies. Additional measurements and signal averaging could have reduced this discrepancy; however, in practice, measurements on the Vevo 770 were time limited because of other demands on the machine and a need to keep scan time within accepted costs. Future studies will address these issues.

Also, the NPL setup allowed for repeat measurements to be made at the same position on the sample. Sample placement in the Vevo 770 setup was changed between measurements, accounting for the greater range of measured values.

It should be noted that the IEC guidelines are specifically for the frequency range 2 to 10 MHz, and as yet, there are no guidelines for higher frequencies.

An additional uncertainty arises from the measurement of the thickness of the TMM. For the NPL measurements, a micrometer was used to measure thickness at multiple locations around the center of the TMM, and the variation was found to be < 0.1 mm. This variation could be due to unevenness in the surface of the TMM or to measurement errors resulting from the compressibility of the TMM. For the Vevo 770 measurements, a time-of-flight method was used to determine cell thickness at each measurement location. This method was originally used to describe a tissue sample without a protective membrane and with the assumption that all frequency components have the same amplitude and phase shift. The measured variation was found to be ± 0.2 mm and in agreement with caliper measurements. The layer of glycerol solution that provided acoustic coupling to the Saran wrap within the cell will also have affected the calculated thickness, although this is estimated as small compared with the uncertainties in the thickness measurements of the TMM ($\ll 0.1$ mm) because of the spreading to all sides of the TMM cell and the loss of some of the solution when sealing the cell with a second layer of Saran wrap. The measure of attenuation for the NPL system required measurements of two thicknesses of the TMM (eqn [5]). The combined uncertainty is estimated to be 0.1 mm from the micrometer measurements of the two different thicknesses of the TMM samples, resulting in the uncertainties seen in Figure 5. A more accurate measurement of thickness may reduce the discrepancy.

The Saran wrap interfaces on the test cells will also affect the uncertainty in the attenuation values, although corrections have been applied accordingly. The greater variation in the water bath temperature of the Vevo 770 measurements (± 1°C vs. ± 0.1°C) will also have caused greater variation in the measurements.

Note that in accordance with the original recipe, this TMM does not have any preservative agent and is therefore not suitable for long-term use.

CONCLUSIONS

In this study, two independent methods of assessing important acoustic properties were carried out on a TMM that had been employed in a previous study as a mechanically more resilient alternative to the commonly used IEC agar-based TMM, in which the speed of sound and attenuation were reported only at a frequency of 5 MHz. Our aim was to extend these measurements into a higher-frequency range (5 to 60 MHz), and therefore it could now be useful for preclinical ultrasound applications. A stronger TMM will have applications in designing phantoms for preclinical systems, for example, in creating wall-less flow phantoms or complex geometries (Meagher et al. 2007).

Acknowledgments—The authors gratefully thank Dr. Jacinta Browne (Dublin Institute of Technology, Dublin, Ireland) for preliminary measurements and useful discussions. We are grateful to Professor Tamie Poepping (University of Western Ontario, Canada) for advice on the TMM preparation and to Dr. Chao Sun for advice on test cell construction. We also thank Mr Stan Loneskie (Edinburgh Royal Infirmary, UK) for the supply and construction of the PVC rings.

REFERENCES

American Institute of Ultrasound in Medicine (AIUM). Methods for specifying acoustic properties of tissue mimicking phantoms and objects, Stage 1. Laurel, MD: Author; 1995.

Brewin MP, Pike LC, Rowland DE, Birch MJ. The acoustic properties, centered on 20 MHZ, of an IEC agar-based tissue-mimicking material and its temperature, frequency and age dependence. Ultrasound Med Biol 2008;34:1292–1306.

Browne JE, Ramnarine KV, Watson A, Hoskins PR. Assessment of the acoustic properties of common tissue-mimicking test phantoms. Ultrasound Med Biol 2003;29:1053–1060.

Cannon LM, Fagan AJ, Browne JE. Novel tissue mimicking materials for high frequency breast ultrasound phantoms. Ultrasound Med Biol 2011;37:122–135.

Del Grosso VA, Mader CW. Speed of sound in pure water. J Acoust Soc Am 1972;52:1442–1446.

Foster FS, Mehi J, Lukacs M, Hirson D, White C, Chaggares C, Needles A. A new 15–50 MHz array-based micro-ultrasound scanner for preclinical imaging. Ultrasound Med Biol 2009;35:1700–1708.

Goertz D, Joanne L, Kerbel R, Burns P, Foster F. High-frequency Doppler ultrasound monitors the effects of antivascular therapy on tumor blood flow. Cancer Res 2002;62:6371–6375.

He P. Measurement of acoustic dispersion using both transmitted and reflected pulses. J Acoust Soc Am 2000;107:801–807.

Hoskins PR. Simulation and validation of arterial ultrasound imaging and blood flow. Ultrasound Med Biol 2008;34:693–717.

Hoskins PR. Estimation of blood velocity, volumetric flow and wall shear rate using Doppler ultrasound. Ultrasound 2011;19:120–129.

International Electrotechnical Commission (IEC). Ultrasonics—Flow measurement systems—Flow test object. Geneva: IEC Publ; 2001. p. 61685.

King DM, Moran CM, McNamara JD, Fagan AJ, Browne JE. Development of a vessel-mimicking material for use in anatomicly realistic Doppler flow phantoms. Ultrasound Med Biol 2011;37:813–826.

Kuo IY, Hete B, Shung KK. A novel method for the measurement of acoustic speed. J Acoust Soc Am 1990;88:1679–1682.

Madsen EL, Frank GR, Carson PL, Edmonds PD, Frizzell LA, Herman BA, Kremkau FW, O'Brien WD, Parker KJ, Robinson RA. Interlaboratory comparison of ultrasonic attenuation and speed measurements. J Ultrasound Med 1986;5:569–576.

Madsen EL, Frank GR, Dong F. Liquid or solid ultrasonically tissue-mimicking materials with very low scatter. Ultrasound Med Biol 1998;24:535–542.

Meagher S, Poepping TL, Ramnarine KV, Black RA, Hoskins PR. Anatomic flow phantoms of the nonplanar carotid bifurcation: Part II. Experimental validation with Doppler ultrasound. Ultrasound Med Biol 2007;33:303–310.

Moran CM, Pye SD, Ellis W, Janeczko A, Morris KD, McNeilly AS, Fraser HM. A comparison of the imaging performance of high resolution ultrasound scanners for preclinical imaging. Ultrasound Med Biol 2011;37:493–501.

O'Donnell M, Jaynes E, Miller J. Kramers–Kronig relationship between ultrasonic attenuation and phase velocity. J Acoust Soc Am 1981;69: 696–701.

Pinkerton JMM. The absorption of ultrasonic waves in liquids and its relation to molecular constitution. Proc Phys Soc B 1949;62:129–141.

Rajagopal S, Sadhoo N, Zeqiri B. Reference characterisation of sound speed and attenuation of the IEC agar-based tissue-mimicking material up to a frequency of 60 MHz. Ultrasound Med Biol 2014; In proof http://dx.doi.org/10.1016/j.ultrasmedbio.2014.04.018.

Ramnarine KV, Anderson T, Hoskins PR. Construction and geometric stability of physiologic flow rate wall-less stenosis phantoms. Ultrasound Med Biol 2001;27:245–250.

Rickey DW. A wall-less vessel phantom for Doppler ultrasound studies. Ultrasound Med Biol 1995;21:1163–1176.

Ryan LK, Foster F. Tissue equivalent vessel phantoms for intravascular ultrasound. Ultrasound Med Biol 1997;23:261–273.

Steel R, Fish PJ. Velocity fluctuation reduction in vector Doppler ultrasound using a hybrid single/dual-beam algorithm. IEEE Trans Ultrason Ferroelectr Freq Control 2003;50:89–93.

Sun C, Pye SD, Browne JE, Janeczko A, Ellis B, Butler MB, Sboros V, Thomson AJW, Brewin MP, Earnshaw CH, Moran CM. The speed of sound and attenuation of an IEC agar-based tissue-mimicking material for high frequency ultrasound applications. Ultrasound Med Biol 2012;38:1262–1270.

Szabo TL. Causal theories and data for acoustic attenuation obeying a frequency power law. J Acoust Soc Am 1995;97:14–24.

Teirlinck CJ, Bezemer RA, Kollmann C, Lubbers J, Hoskins PR, Ramnarine KV, Fish PJ, Fredeldt KE, Schaarschmidt UG. Development of an example flow test object and comparison of five of these test objects, constructed in various laboratories. Ultrasonics 1998; 36:653–660.

Wear K, Stiles T, Frank G, Madsen E, Cheng F, Feleppa E, Hall CS, Kim BS, Lee P, O'Brien WD Jr, Oelze ML, Raju BI, Shung KK, Wilson TA, Yuan J. Interlaboratory comparison of ultrasonic backscatter coefficient measurements from 2 to 9 MHz. J Ultrasound Med 2005;24:1235–1250.

Wells PNT. Ultrasound imaging. Phys Med Biol 2006;51:R83–R98.

Wu J. Determination of velocity and attenuation of shear waves using ultrasonic spectroscopy. J Acoust Soc Am 1996;99: 2871–2875.

Xu X, Sun L, Cannata JM, Yen JT, Shung KK. High-frequency ultrasound Doppler system for biomedical applications with a 30-MHz linear array. Ultrasound Med Biol 2008;34:638–646.

Yang X, Hollis L, Adams F, Khan F, Hoskins PR. A fast method to estimate the wall shear stress waveform in arteries. Ultrasound 2013; 21:23–28.

Zeqiri B, Bickley CJ. A new anechoic material for medical ultrasonic applications. Ultrasound Med Biol 2000;26:481–485.

Zeqiri B, Scholl W, Robinson SP. Measurement and testing of the acoustic properties of materials: A review. Metrologia 2010b;47: S156–S171.